Chapter 5
Sealing of Surface Micromachined Poly-SiGe Cavities

This chapter describes the sealing of polycrystalline SiGe (poly-SiGe) surface micromachined cavities for above-CMOS pressure sensor applications. Two different sealing techniques involving thin-film deposition are investigated: direct sealing and sealing by using an intermediate porous layer. The sealing materials studied include Si-oxide and aluminum. Both μc-SiGe and SiC are evaluated as porous layer. The maximum processing temperature is kept below 460 °C to allow for the post-processing on top of standard CMOS. Section 5.1 gives a short overview about the most common sealing methods for pressure sensors and lists the main requirements the sealing layer needs to fulfill. Section 5.2 explains the fabrication process of the test structures. The measurement set up used to characterize the deflection of the sealed membranes deflection under different applied loads is introduced in Sect. 5.3. In Sect. 5.4 the theoretical analysis of the load-deflection behavior of square membranes is introduced, and with the help of finite element simulations a model adapted to our test structures is developed. Section 5.5 gives the results of the short- and long-term hermeticity tests performed on the sealed membranes. This section also describes the use of micro-venting holes drilled using Focus Ion Beam (FIB) in some of the sealed membranes to study the behavior of the diaphragms under 0-pressure-difference. This chapter ends with a conclusion (Sect. 5.6) listing the main aspects of the different sealing techniques studied and the reasons behind the selection of SACVD (Sub-Atmospheric Chemical Vapor Deposition) oxide as sealing layer for our pressure sensor.

5.1 Introduction

Sealed cavities are crucial components in many micromachined applications, such as for packaging MEM components or for producing pressure sensors. For pressure sensors the sealed cavity supplies a reference for pressure measurements. In general there are two techniques for microcavity sealing: wafer bonding (used, for example,

P. González Ruiz et al., *Poly-SiGe for MEMS-above-CMOS Sensors*,
Springer Series in Advanced Microelectronics 44, DOI: 10.1007/978-94-007-6799-7_5,
© Springer Science+Business Media Dordrecht 2014

in silicon pressure sensors) and thin-film deposition (typically employed in surface micromachined pressure sensors).

In wafer bonding, a cap wafer (silicon, glass or ceramic) is bonded to the MEMS wafer by using either direct bonding or by bonding with an intermediate layer, creating a hermetically sealed cavity [1]. Wafer bonding techniques, even though well established and commercialized, are costly because they require a second substrate, careful alignment of the two parts, double the thickness of the chip and need a large area for the sealing frame. Moreover the high temperatures, high voltages and/or high pressures involved may affect the performance of the encapsulated device or the properties of the sensor membrane and therefore its performance.

In the second sealing technique the membrane layer is deposited on top of a sacrificial material. Access holes or channels are provided in the membrane to remove the sacrificial material and to create a cavity underneath. For release, horizontal (placed on the cavity sides) or vertical (on the membrane) access channels can be used. After release, the access holes are typically sealed by thin film deposition. Compared with wafer bonding, sealing by the deposition of a thin-film has several advantages:

1. It eliminates the need for aligning two wafers and the challenges of bonding on processed (i.e. not smooth) surfaces.
2. It reduces the topography and reduces the width of the required sealing ring, allowing for smaller devices.
3. It eliminates the need for high temperatures, pressures or voltages usually employed in wafer bonding.

Sealing of microcavities by thin-film deposition was first demonstrated by Guckel in [2], using LPCVD (Low Pressure CVD) polysilicon deposition to seal a poly-Si cavity. Since then great efforts have been made on sealing of surface micromachined cavities by CVD deposition of thin films. Besides poly-Si also LPCVD Si-nitride was used to successfully seal surface micromachined cavities [3, 4]. These CVD materials however require high deposition temperatures, typically above 700 °C, and are therefore not suitable for post processing of the MEMS above the CMOS circuitry. Different alternatives with lower process temperatures have been proposed in the last years. Liu [5] studied the use of LPCVD phosphosilicate glass (PSG) at 450 °C and PECVD (Plasma Enhanced CVD) Si-nitride at 300 °C for the sealing of poly-Si microcavities with lateral release holes. These low temperature sealing materials were however found to be inefficient since relatively thick layers were required to successfully seal the cavities. Alternatively, Al evaporation has been used to vacuum seal poly-Si cavities [6]. Recently sputter-deposited AlCu in combination with a μc-SiGe porous cover on top of the release holes was used to hermetically seal poly-SiGe cavities for thin-film packaging applications [7]. A modified version of this sealing process has been used to hermetically encapsulate SOI resonators[8].

The main requirements for pressure sensor sealing by thin film deposition can be enumerated as follows:

1. A low minimum required thickness of the sealing layer. Sealing occurs when the deposited thickness of sealing material reaches a threshold. In pressure sensor devices the sealing layer becomes an integral part of the cavity diaphragm, contributing to its overall thickness. A small threshold thickness is therefore desirable to avoid degradation of the sensor sensitivity. A thin sealing layer also leads to less bi-material effects and ensures that the average membrane properties are close to those of the preferred structural material (in our case, SiGe).
2. A low sealed-in pressure. The expansion of the gasses trapped inside the cavity with increasing temperature will degrade the temperature dependence of the pressure sensors performance. Therefore it is, in general, preferred to have a vacuum-sealed cavity for pressure sensor applications as this will minimize the trapped gas effects.
3. A low (residual) tensile stress. The residual stress of the sealing layer will contribute to the overall stress of the diaphragm, altering the sensor membrane response. In general, the higher the tensile stress in the diaphragm, the lower the membrane deflection for a certain pressure difference. A diaphragm with compressive stress will, on the other hand, deflect more, but it has the potential for buckling. A zero or marginally tensile residual stress will minimize the effect of the sealing layer.
4. The coefficient of thermal expansion (CTE) of the sealing layer should close to that of the sensor membrane since thermal shock or thermal cycling may cause membrane cracking and delamination if the materials are not matched.

For the fabrication of the pressure sensor two different approaches for the sealing of poly-SiGe cavities by thin film deposition were investigated. The first approach consists simply in direct sealing of the released cavities by deposition of different kinds of CVD (Chemical Vapor Deposition) Si-oxide or AlCu. In the second approach the sacrificial oxide release is done through an intermediate porous cover. This porous cover has two main functions: it prevents deposition of sealing material inside the cavity and it reduces the required thickness of the sealing layer. Two different materials were investigated as porous cover: SiC and μc-SiGe [9]. The use of Si-oxide, AlCu (and SiGe in the literature) for the sealing of cavities released through a porous cover was studied. The next section describes in detail the fabrication process of the sealed test structures.

5.2 Fabrication Process

The test structures consist of free-standing poly-SiGe membranes covering 3 μm-deep cavities. Poly-SiGe membranes with different areas (200×200, 250×250, 300×300 and 500×500 μm^2) and thicknesses (from 2 up to 8.5 μm) were fabricated. The general fabrication process for the test structures with a 3.5 μm thick membrane and sealed without intermediate porous layer is schematically illustrated in Fig. 5.1. The fabrication process for the test structures released and sealed using

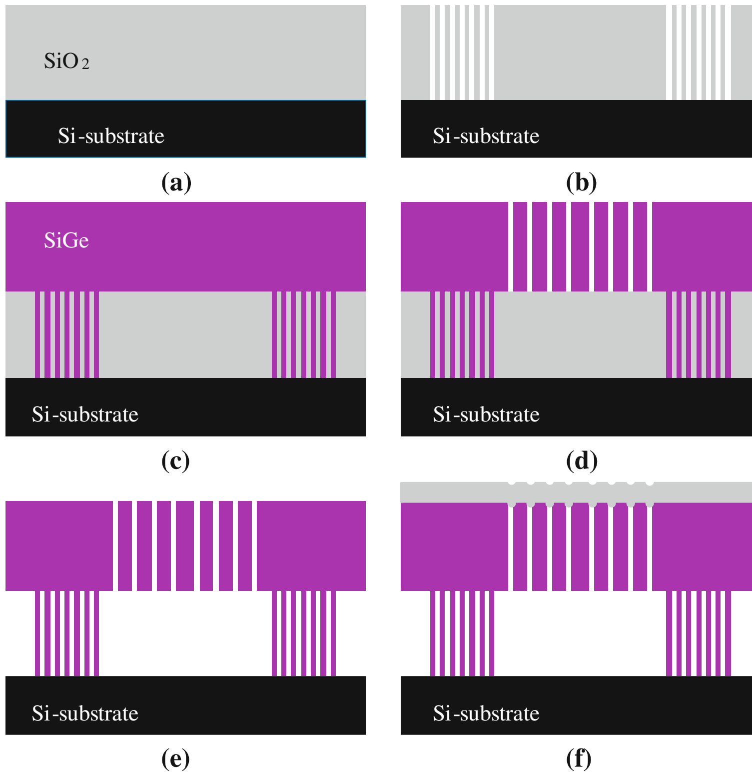

Fig. 5.1 Schematic process flow. **a** Deposition of sacrificial oxide on a Si-wafer. **b** Patterning of the oxide to define the anchors. **c** Deposition of poly-SiGe structural layer. **d** Opening of the release holes in the membrane. **e** Etching of the sacrificial oxide by vHF. **f** Sealing

an intermediate porous cover is slightly more complex and will be explained in the corresponding subsection. Test structures with a membrane thickness different from 3.5 μm do not have anchors (see also further).

A standard 8-in-diameter Si (100) wafer is used as starting substrate. We first deposit a 3 μm-thick HDP oxide layer to be used as sacrificial material. To define the anchor region trenches were etched in the sacrificial oxide, stopping in the underlying Si substrate, and filled with poly-SiGe. The chosen anchor design consists of crossing vertical and horizontal anchor lanes, as depicted in Fig. 5.2. The total anchor region surrounding each membrane is 25 μm for all the test structures. However only the 3.5 μm-thick membranes had patterned anchors. For the rest of membranes the SiGe structural layer is deposited over unpatterned oxide (see Table 5.1).

The poly-SiGe structural layer was then deposited at 460°C chuck temperature (450 °C wafer temperature) in an Applied Materials (AMAT) PECVD CxZ chamber, mounted on an AMAT Centura Giga-Fill SACVD platform. All the layers, except for the thinner membranes, were deposited by a combination of CVD and PECVD

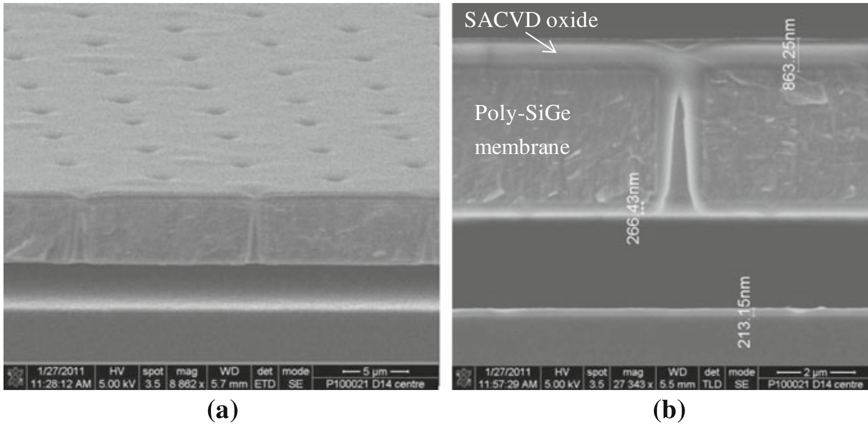

Fig. 5.2 **a** *Top* and **b** Cross-section SEM picture of a poly-SiGe membrane sealed with SACVD. During sealing with 900nm SACVD Si-oxide, ∼270 nm of oxide is deposited on the inner side of the membrane while ∼220 nm of oxide is deposited at the *bottom* of the cavity

Table 5.1 Process parameters for the different sealing methods considered

Sealing technique	Sealing material	SiGe membrane thickness (μm)	Temp. (°C)	Pressure (kPa)	Anchor
Direct sealing	SACVD Si-oxide	3.5	420	60	Yes
	HDP Si-oxide	3.5	∼400	NA	Yes
	PECVD Si-oxide	3.5	400	0.35	Yes
	AlCu	8.5	350	0.001	No
Porous layer	HDP Si-oxide	3.5	400	NA	Yes
	AlCu	2	350	0.001	No

The SiGe membrane thickness for the corresponding test structure employed is also indicated

B-doped SiGe depositions with 30 seconds CF_4 clean at the PECVD/PECVD interfaces [10], similar as the poly-SiGe structural layer in the pressure sensor fabrication process (Chap. 4). The silicon gas source is pure silane, whereas 10% germane in hydrogen has been used as the germanium gas source. Three different poly-SiGe thicknesses are considered in this study. After deposition, a CMP (Chemical Mechanical Polishing) process is applied to planarize and smooth the poly-SiGe membrane surface. This CMP step was not included during the processing of the 2 μm-thick membranes. The final poly-SiGe stack build-up and thickness (estimated from cross-section pictures) is:

- For a 2 μm thick-membrane: a 2 μm thick PECVD SiGe layer without preceding crystalline CVD seed layer.
- For a 3.5 μm thick-membrane: a stack of a thin (∼400nm) CVD SiGe seed layer and 2 PECVD SiGe layers.
- For a 8.5 μm thick-membrane: a stack of a thin CVD SiGe seed layer and 5 PECVD SiGe layers.

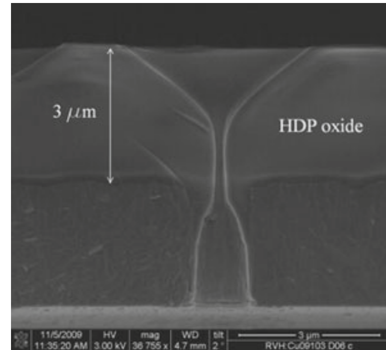

Fig. 5.3 Sealing of a release hole with HDP oxide. A thickness of 3 μm is not enough to completely close the hole.

It is important to clarify that not all the test structures here described were fabricated specifically for the development of the pressure sensor process flow. The test structures with 2 μm thick or 8.5μm thick membranes were intended for the development of the packaging flow (work described in [11]). Hence the different membrane thicknesses and deposition processes.

After deposition, the poly-SiGe structural layer was patterned and plasma-etched to open the release holes. A symmetrical pattern of square release holes of 1×1 μm^2 with a maximum spacing of 9.5 μm was used (see Fig. 5.3). The final size of the release holes after etch is $\sim1.2\times1.2$ μm^2. All sacrificial oxide inside the cavities is removed by a combination of anhydrous vapor HF (AVHF) and ethanol vapor on a Primaxx CET tool. More information about the release process can be found in Chap. 4. After release the membranes are sealed. Table 5.1 contains the main process parameters for the different sealing materials considered.

5.3 Direct Sealing

5.3.1 Sealing with Si-Oxide

Si-oxide is an interesting sealing material for piezoresistive pressure sensor applications as it can be used simultanously as an isolation layer between membrane and piezoresistors. One drawback, however, is that oxide has a typical CTE ten times smaller than that of the poly-SiGe membrane (0.5 ppm/°C versus the 5 ppm/°C for the SiGe). This CTE mismatch may give rise to severe thermal stresses during the manufacturing of the pressure sensor and will compromise the temperature stability of the sensor.

Three different kinds of CVD (Chemical Vapor Deposition) oxide were considered as sealing layer: SACVD (Sub-Atmospheric CVD) Si-oxide, HDP (High Density Plasma) Si-oxide and PECVD (Plasma-Enhanced CVD) Si-oxide. In a CVD chamber conformal deposition occurs: the material is deposited on the top and bottom surfaces

of the diaphragm, the substrate and on the sidewalls of the release holes. Sealing occurs when the oxide deposited on opposite walls of the release holes meet in the center once a threshold thickness is reached [5].

- *Sealing with SACVD oxide:* The first sealing material studied is SACVD Si-oxide deposited by a reaction between TEOS ($Si(OC_2H_5)_4$ or Tetraethyl Orthosilicate) and ozone (O_3). During the reaction byproducts such as water vapour and ethylene are formed. A 900 nm-thick SACVD oxide layer was deposited at 420 °C and a pressure of 60 kPa on top of the released poly-SiGe membranes. From Fig. 5.2 we can see that the $1.2 \times 1.2\ \mu m^2$ release holes could be successfully sealed with a 900 nm-thick SACVD oxide. The top surface of the sealed membrane (Fig. 5.2b) is very smooth which is important to avoid adhesion and lithography problems during further processing. However, during the sealing process around 400 nm of oxide was deposited inside the cavity For thin film packaging, the deposition of sealing material inside the cavities is a concern since it will deposit on the surfaces of the packaged device, altering the device characteristics. This is not an issue for piezoresistive pressure sensors. On the other hand, for pressure sensors the thickness of the deposited material inside the cavity will reduce the cavity depth and might therefore reduce the full working pressure range of the devices.
- *Sealing with HDP oxide:* The second oxide sealing method considered employs HDP Si-oxide deposited by CVD based on a reaction between silane (SiH_4) and oxygen. The deposition temperature is not monitored, but it is expected to be around 400 °C. The process pressure is also not controlled as the throttle valve is fully opened during the chemical reaction. However, it is expected to be lower than the 60 kPa pressure used for the SACVD oxide deposition. Because of the non-conformal plasma-based process, very thick layers are required in order to seal release holes of $1.2 \times 1.2\ \mu m^2$ directly with HDP oxide (Fig. 5.3). This can be a benefit for thin film packaging applications as it results in more robust membranes, but it is not ideal for pressure sensors applications since a thicker membrane results in a lower sensitivity. For this reason the use of HDP Si-oxide for the direct sealing of the poly-SiGe pressure sensors was discarded.
- *Sealing with PECVD oxide:* The third oxide considered as sealing material is PECVD Si-oxide deposited by a reaction between silane and nitrous oxide (N_2O). Ammonia (NH_3) is a byproduct. The deposition of PECVD oxide is carried out at a low pressure (only 350 Pa), making it an interesting material for near-vacuum sealing of surface micromachined cavities for pressure sensors or thin-film packaging sealing. Figure 5.4 shows a cross-section picture of a 3.5 μm-thick poly-SiGe released membrane sealed with 3 μm of PECVD oxide. From this Figure it seems that to succesfully seal the $1.2 \times 1.2\ \mu m^2$ release holes around 2 μm of PECVD oxide could already have been enough. Similar as HDP oxide, PECVD oxide is also a non-conformal plasma-based process. Because of this the required thickness to seal the membranes is larger than in the case of SACVD Si-oxide. On the other hand, the quantity of material deposited inside the cavity is drastically reduced compared to SACVD sealing.

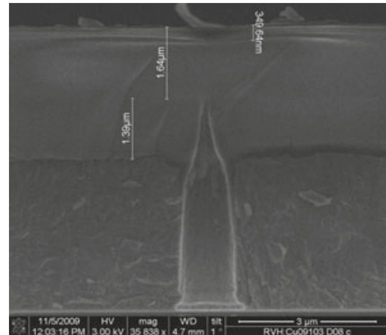

Fig. 5.4 Sealing of a release hole with 3µm thick PECVD oxide. From this picture it seems that the minimum required thickness to seal the release holes is 1.5 µm < ts < 3 µm.

From these results we can conclude that the most efficient CVD Si-oxide layer for direct sealing of the poly-SiGe cavities is SACVD Si-oxide, followed by PECVD Si-oxide. HDP Si-oxide resulted to be the most inefficient for direct sealing as a very thick layer (thicker than 3 µm) is necessary to succesfully seal the release holes. Only SACVD Si-oxide will be further evaluated as sealing layer.

For pressure sensor applications, not only a low minimum required thickness is important, but also the residual stress of the sealing layer needs to be considered. The stress of the SACVD Si-oxide layer was determined from the measured wafer curvature after film deposition by applying Stoney's equation [12]. A 300 nm-thick SACVD oxide layer deposited on blanket Si wafers was used for the measurements. The stress was measured as deposited, three days, and a week after the deposition (Fig. 5.5). The initial stress of the as deposited film was 335 MPa (tensile) but it decreases over time, probably due to absorption of moisture from the air [13]. According to [13], the residual stress of a SACVD Si-oxide film will also change after annealing steps and can be tuned to a value from tensile to compressive depending on annealing temperature and ambient gas.

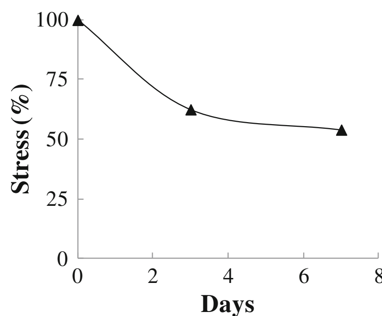

Fig. 5.5 Stability over time of the residual stress of a SACVD layer deposited on a blanket wafer. After one day the stress of the film dropped to 62.5 % of the initial as-deposited value, although the decrease in the following days was not so steep. After 7 days the stress was ∼50 % of the initial value

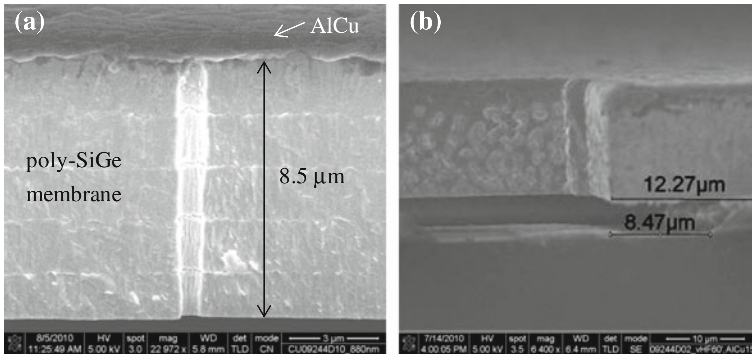

Fig. 5.6 **a** Direct sealing of a 8.5 µm-thick poly-SiGe membrane with 1.5 µm of AlCu. The interface between the five PECVD SiGe layers is visible. **b** Strong reaction between the SiGe and AlCu is visible

5.3.2 Sealing with AlCu

AlCu is a potential candidate for vacuum sealing of surface micromachined cavities due to its low deposition pressure (1 Pa). In this work the use of sputter-deposited AlCu (0.5 wt%) for the direct sealing of poly-SiGe microcavities is investigated. To limit the required AlCu thickness for direct sealing, the size of the printed release holes was reduced to $0.8 \times 0.8\ \mu m^2$ (final size after etch is $\sim 0.95 \times 0.95\ \mu m^2$). Figure 5.6a shows a cross-section picture of a 8.5 µm thick poly-SiGe membrane sealed with a 1.5 µm thick AlCu layer. The stress of the AlCu layer, as determined from wafer bow [12], is ∼100MPa tensile. Similar as the SACVD oxide, this stress can also relax with time [14]. From Fig. 5.6b it seems there is a strong reaction between the SiGe and the AlCu (there is no barrier layer), which may alter the properties and thus also the stress of the sealed membrane.

5.4 Intermediate Porous Cover

In this section the use of a porous cover on top of the release holes to prevent sealing material deposition inside the cavity and reduce the minimum required thickness of the sealing layer is discussed. In order to limit the effect of this (locally) porous layer on the thermal behaviour of the sealed membrane, it is preferred to use a layer with a thermal expansion coefficient (CTE) close to that of the poly-SiGe membrane. Since this porous cover could eventually be used as isolation between the poly-SiGe piezoresistors and the poly-SiGe membrane in the pressure sensor process flow, it must be a non-conductive layer. Two materials to be used as porous cover were considered: PECVD SiC and undoped PECVD microcrystalline (µc) SiGe. The process steps to create this porous cover are illustrated in Fig. 5.7. Similar

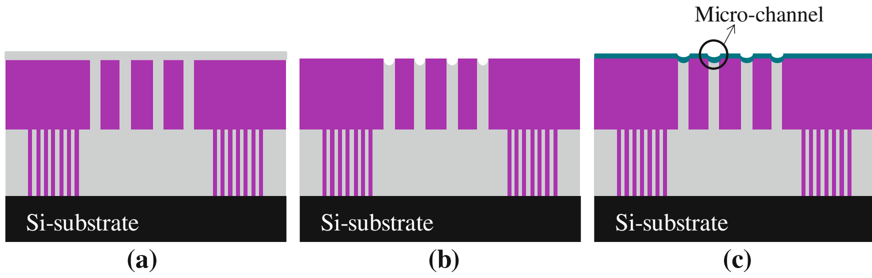

Fig. 5.7 **a** Oxide filling of the release holes, **b** oxide dry recess and **c** porous cover deposition. Micro-channels, with a dimension significantly smaller than 100 nm, are formed above the release holes during the non-conformal deposition of the porous cover

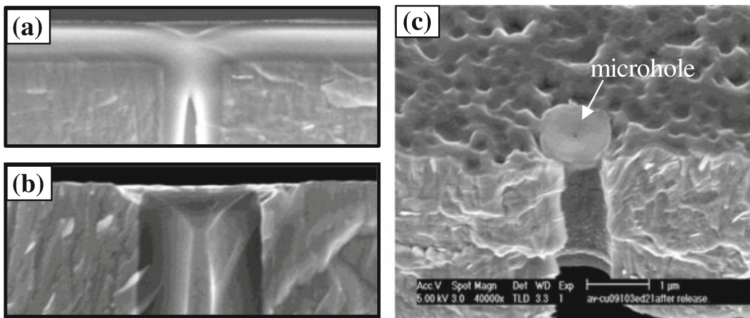

Fig. 5.8 Cross-section SEM pictures of **a** oxide filling and **b** planarized surface after oxide etch back. **c** *Top* SEM picture of a microhole in the porous cover on top of a release hole

processing to form a porous cover on the membrane was already demonstrated in [7, 11]. Up to the opening of the release holes in the poly-SiGe membrane the fabrication flow of these tests structures is equivalent to the one showed in Fig. 5.1. After filling of the release holes with oxide, a dry etch is performed stopping on the SiGe membrane. This etch process creates a small recess in the filling oxide. A thin porous cover, with microchannels above the release holes (Fig. 5.8), is then deposited. All sacrificial oxide inside the cavity is etched by vHF (using the same recipe as for the direct sealed membranes) through the local microchannels in the porous cover. The presence of the porous cover does not affect the vHF Si-oxide etch rate [7]. After release the membranes can be sealed by thin film deposition.

The work on the PECVD SiC porous cover is described in Appendix C. As this material needed a thin Ti adhesion layer, it was ultimately not used for creating sealed cavities as this Ti layer could short-circuit the cavity membrane and the bondpads. The rest of this paragraph therefore deals with the work on μc-SiGe porous covers.

As mentioned before, the porous layer can eventually be used as isolation layer between the poly-SiGe piezoresistors and the poly-SiGe membrane. For this reason, a recipe to deposit a 200 nm-thick undoped μc-SiGe layer using a PECVD process

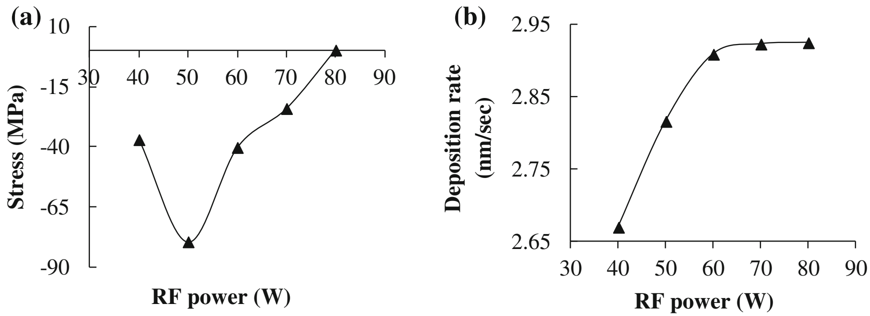

Fig. 5.9 Effect of RF power on residual stress **a** and deposition rate **b** for a 200 nm-thick PECVD μc-SiGe layer. The μc-SiGe layer is deposited on oxide covered Si wafers

was developed specifically for this application. In order to limit the impact of this porous layer on the overall stress of the sealed membrane, a marginally tensile stress was targeted. By increasing the RF power from 40 to 80 W the residual stress in the layer (Fig. 5.9a) could be tuned from compressive to marginally tensile (~0.3 MPa). The stress was calculated from the wafer curvature after deposition of the SiGe film on blanket Si wafers covered with oxide. An increase in RF power also translated into an increase in the deposition rate (Fig. 5.9b).

One advantage of using μc-SiGe as porous layer instead of SiC is that it eliminates the need of a "glue" layer (such as the conductive Ti layer in the case of a porous SiC cover, described in Appendix C) to improve adhesion to the SiGe membrane. Moreover, the use of a single μc-SiGe porous cover instead of the stack Ti/SiC will minimize the negative effects of thermally induced stresses due to CTE mismatch. Also, the marginally tensile stress of the optimized recipe makes μc-SiGe a much more attractive candidate than the Ti/SiC composite layer. For all these reasons μc-SiGe is the selected porous cover.

Two different layers to seal the poly-SiGe cavities released through a porous μc-SiGe were studied:

- 1 μm-thick HDP oxide layer (Fig. 5.10a)
- 690 nm-thick AlCu layer (Fig. 5.10b).

In the case of the HDP oxide, a 3.5 μm-thick sige membrane was used while to investigate AlCu as sealing layer, a 2 μm-thick membrane without patterned anchors was used. A colleague in imec studied the use of PECVD SiGe as sealing material for poly-SiGe cavities used in MEMS packaging [11]. In his work, 2 μm-thick poly-SiGe membranes released through a porous μc-SiGe cover and without patterned anchors were used. The porous μc-SiGe used as cover was a conductive layer, different from the μc-SiGe porous cover used in this work. Figure 5.10c shows SEM pictures of such membranes sealed with PECVD SiGe. We will further analyze the results obtained in [11] for the PECVD SiGe sealed-membranes and compare the results

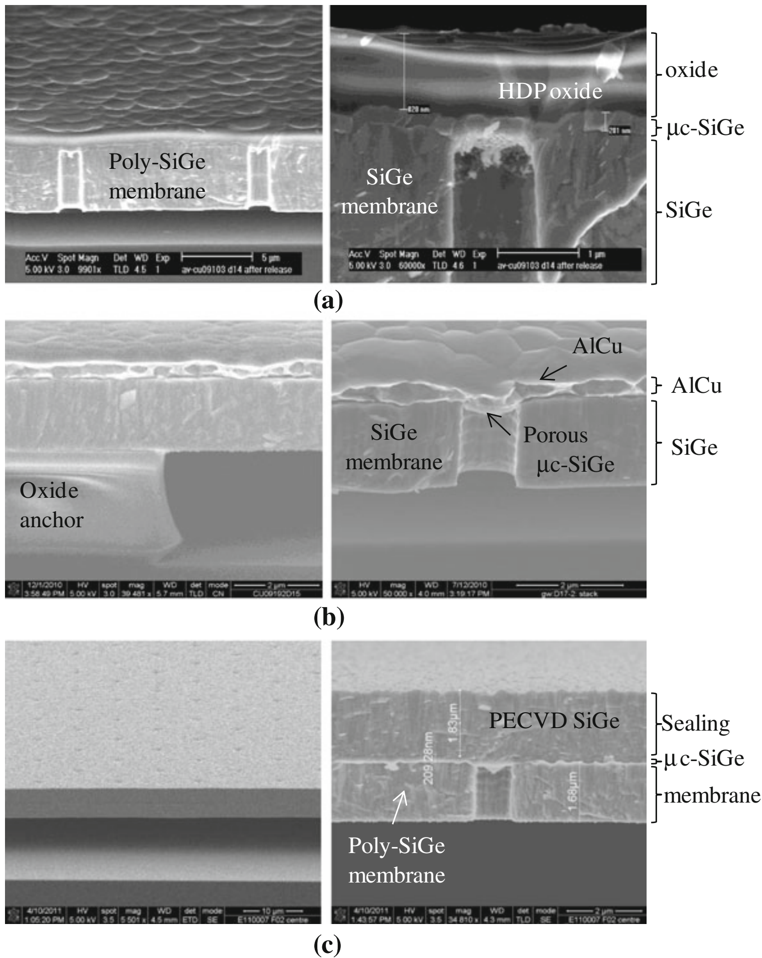

Fig. 5.10 Poly-SiGe membranes released through a µc-SiGe porous cover and sealed with: **a** HDP oxide, **b** AlCu and **c** PECVD SiGe [11]. In **b**, the porous mc-SiGe cover is difficult to appreciate

to those obtained in this work for the HDP Si-oxide and the AlCu sealed poly-SiGe membranes.

In the case of the HDP Si-oxide sealed membranes, a final lithography step operation, followed by the etching of the HDP Si-oxide and the µc-SiGe cover (Fig. 5.11) was performed after sealing. The purpose of this patterning of the sealing layer was to check the effect of an exposed membrane/sealing layer interface on hermeticity. This final processing step was not performed for cavities sealed by any of the other sealing methods considered in this work.

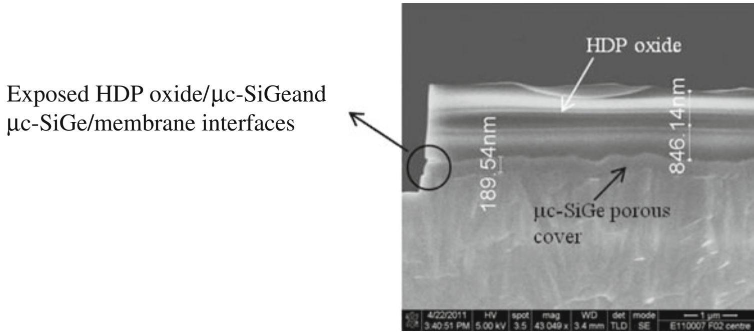

Fig. 5.11 Close view of the exposed interfaces (HDP Si-oxide/μc-SiGe and μc-SiGe/membrane) after the final lithography step for a membrane sealed with HDP oxide and released through a porous μc-SiGe cover

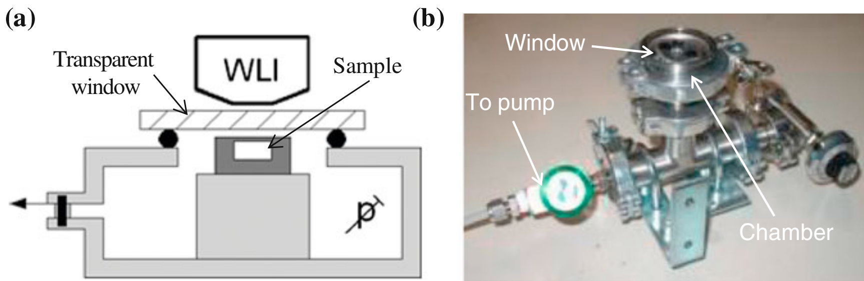

Fig. 5.12 Deflection measurement setup. **a** Schematic—the chamber pressure can be switched between atmosphere (Air) and ∼25 kPa (Vacuum). A glass window is mounted on *top* of the chamber to facilitate the WLI inspection. **b** Photo of chamber—It can be connected to the clean room vacuum system which has a normal pressure of ∼25 kPa

5.5 Measurement Setup

To evaluate the different sealing technologies, the pressure-deflection response of sealed membranes of different dimensions was measured by WLI (White Light Interferometry) using an optical profilometer system (Wyko NT3300) [15, 16] combined with a Through Transmissive Media (TTM) module [17]. The samples were placed into a small dedicated vacuum chamber with a glass window, which is transparent for the light of the interferometer (Fig. 5.12). The membrane deflection is first measured at atmospheric pressure (101 kPa). Then the pressure inside the chamber is pumped down to ∼25 kPa, and the deflection profile is measured again. A difference in membrane deflection under the two pressures considered would indicate that the membranes are sealed. All measurements were done at room temperature.

From the measured membrane deflection under a known pressure together with the predicted deflection by analytical models and FEM (see also next section), the pressure inside the cavity can be estimated. To do so, it is necessary to measure the

membrane deflection accurately. This poses a problem for the oxide-sealed cavities since Si-oxide is transparent to light. To overcome this limitation, a thin (25 nm) Ti layer was deposited on top of the Si-oxide sealing layer. Due to the small thickness of the added Ti layer compared to the total diaphragm thickness (poly-SiGe membrane plus sealing layer), the effect of this Ti layer on the diaphragm response was considered negligible and not taken into account in the calculations and simulations described in the following sections.

5.6 Analytical Model

Both the overall stress and the cavity pressure of our sealed membranes can be determined using the membrane deflection method [18, 19]. In this technique the deflection of the membrane is measured as a function of applied pressure. By fitting the measurement data to an appropriate equation describing the load-deflection response of the membrane, parameters such as internal stress, Young's modulus and sealed-in pressure can be obtained. Different analytical solutions have been proposed to derive the maximum deflection in the centre of a uniformly loaded clamped membrane. In general the mechanical response of a membrane subjected to an external load is governed by its geometry (thickness, size and shape) and material properties (mainly residual stress, Young's modulus and Poisson's ratio).

Following the variational method, the load-deflection model of a clamped square membrane due to a differential pressure ΔP across the membrane is expressed as [20]:

$$\Delta P = \left[C_r \frac{\sigma_0 t}{L^2} + C_b \frac{E_t^3}{\left(1 - v^2\right) L^4} \right] w_0 + \left[C_s f_s(v) \frac{E_t}{L^4} \right] w_0^3 \tag{5.1}$$

where $\Delta P = P - P_{in}$ is the difference between the applied external pressure (P) and the cavity pressure (P_{in}),w_0 is the centre deflection, L is the membrane side length, t the membrane thickness, $\sigma_0$is the residual stress in the membrane, E the Young's modulus and v is the Poisson ratio. The Poisson ratio dependent function $f_s(v)$is given by [21]:

$$f_s(v) = \frac{1 - 0.271v}{1 - v} \tag{5.2}$$

In (5.1), the first term within the square bracket represents the stiffness of the membrane due to the residual stress while the second term is the stiffness due to bending. The last term represents the stiffness due to nonlinear spring hardening. This model has already been succesfully applied to extract mechanical properties of poly-Si and Si-nitride films [18, 22]. In these references, however, the assumption of $w_o >> t$ (which is not true in our case) was applied and the term describing the stiffness due to bending (second term in first parenthesis) was neglected.

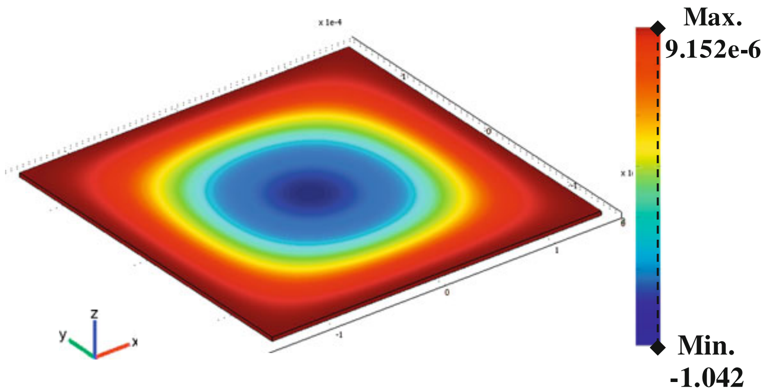

Fig. 5.13 Simulated deflection (in μm) of a poly-SiGe membrane of length L = 300 μm and thickness 3.5 μm subjected to a total differential pressure of 1 bar

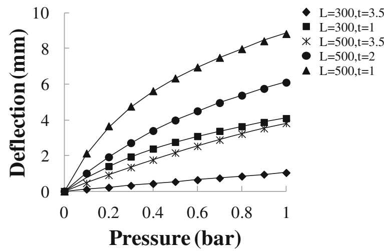

Fig. 5.14 Simulated deflection together with fitting curves from Eq. (5.1) for square poly-SiGe membranes of length (L) and thickness (t) in μm. The markers are FEA simulated values. The *solid lines* represent the fitting curves. The pressure in the x-axis represents the differential pressure across the membrane

The value of the dimensionless constants C_r, C_b and C_s can be obtained by simulating the deflection of square membranes for a sequence of applied loads and fitting the results to Eq. (5.1). To do so, finite element simulations of square suspended membranes of different areas and thicknesses were carried out using the program COMSOL [23] (Fig. 5.13). Clamped edges were implemented as boundary conditions. A Young's modulus $E = 140\,\text{GPa}$, a Poisson's ratio $\upsilon = 0.23$ and a residual stress $\sigma = 70$ MPa for poly-SiGe are used both in the simulations and calculations. Figure 5.14 plots the simulated deflection vs. pressure together with the fitting curves for square poly-SiGe membranes of different dimensions. The modeled values (with accuracy within 3 %) for C_r, C_b and C_s are 15.4, 65.6 and 31.7, respectively. These values are similar to the ones reported in [21] for square membranes with a possion's ratio $\upsilon = 0.25$.

In Eq. (5.1) the effect of the release holes is not included. A factor λ describing the decreased stiffness of the membrane due to the openings was empirically formulated in [24] as:

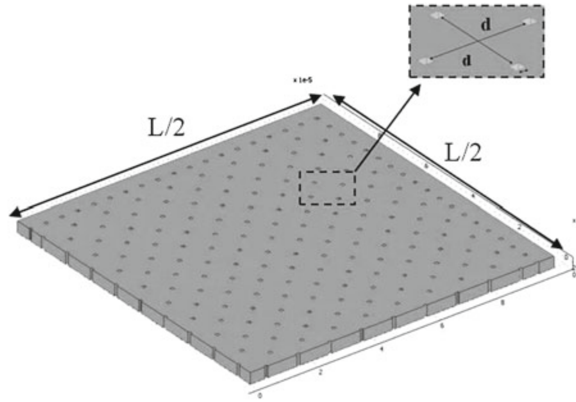

Fig. 5.15 FEA model of a quarter of a membrane of length L. Zoom in the pattern of release holes (d = 9.5 μm)

$$\lambda = 1 - \frac{Area_{openings}}{Area_{total}} \tag{5.3}$$

which yields a value of ~0.975 for all the structures considered in this work. In order to account for the effect of release holes the Young's modulus E in equation (5.1) can be replaced by $E_h = \lambda E$.

For a more accurate estimation of the value of parameter λ, finite element simulations of the load-deflection response of perforated membranes were performed. Square membranes with different lengths (from 50 to 500 μm) and thicknesses (from 0.1 to 3.5 μm) but with the same pattern of release holes (Fig. 5.3) were considered in the simulations. Since the designed structures posses' 4-fold symmetry only a quarter of the model is used in the simulations to reduce computational time (Fig. 5.15). Substituting the simulated deflection at a certain pressure in (5.1) (with E replaced by E_h) and solving the equation in λ, a value of 0.967±0.006 was obtained. This value is very close to the one predicted by (5.3).

5.7 Results and Discussion

As mentioned before, the deflection of the sealed membranes is measured using an optical interference profilometry system under two different applied pressures. Figure 5.16 shows a 3D representation of the optically measured deflection in air (1 bar) of membranes sealed with μc-SiGe porous layer and HDP Si-oxide. Figure 5.17 plots the obtained deflection profiles along the centre of membranes (cut along X in Fig. 5.16) of 500 × 500 μm^2 sealed with AlCu (both as direct sealing and in combination with a porous cover) and SiGe, measured in air (1 bar) and vacuum (0.25 bar). Particularly interesting to note is the deflection profile in air for the membranes sealed with SiGe; such a profile is characteristic of postbuckled membranes under differential pressure [25]. The maximum deflection for membranes of different areas

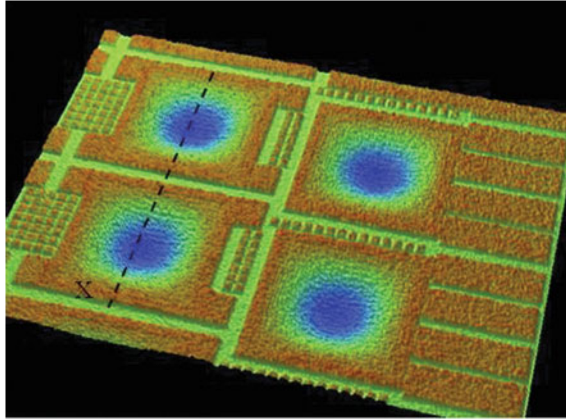

Fig. 5.16 Optical picture of the deflection in air of $300 \times 300\,\mu\text{m}^2$ membranes sealed with HDP Si-oxide

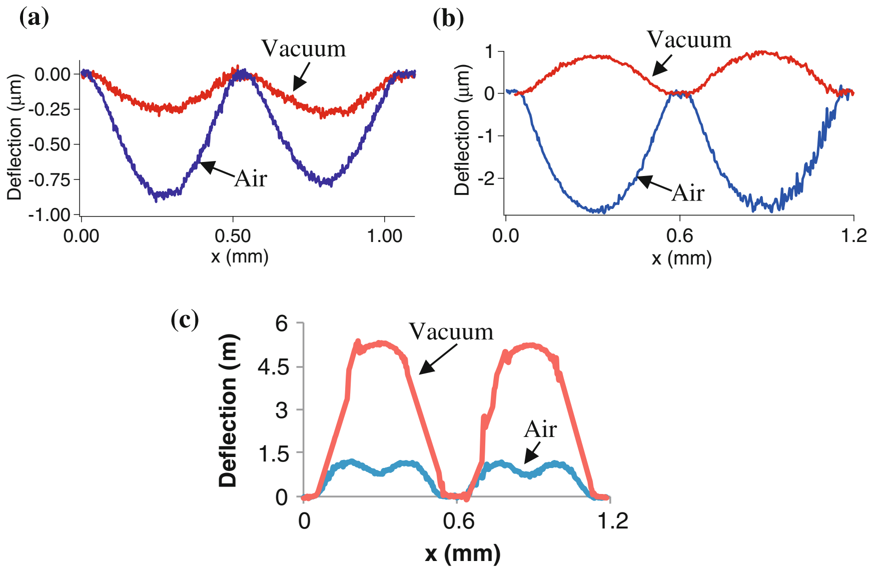

Fig. 5.17 Measured membrane deflection for membranes sealed with **a** AlCu only, **b** µc-SiGe+AlCu and **c** µc-SiGe+SiGe (from [1]). The difference in *deflection* indicates that the membranes are sealed. Each graphs plots the deflection of two identical membranes

(200×200, 250×250 and $300 \times 300\,\mu\text{m}^2$) sealed with (a) SACVD Si-oxide and (b) HDP Si-oxide is shown in Fig. 5.18. From the obtained results we can conclude that all the sealing techniques and materials considered provide short-term hermetic sealing.

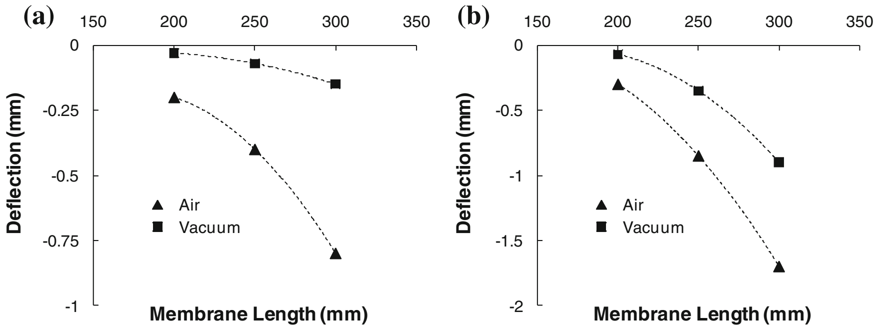

Fig. 5.18 Measured deflections for membranes of different areas: 200 × 200, 250 × 250 and 300 × 300 μm². **a** Membranes sealed with SACVD oxide and **b** μc-SiGe/HDP oxide-sealed membranes

The resulting cavity pressure (P_{in}) and the residual stress (σ_0) of the composite membranes can be determined by fitting the measured load-deflection data to Eq. (5.1). For this method to be applicable, it is necessary to foresee a gap large enough to accommodate the maximum expected deflection of the membrane. An insufficient gap depth would translate into an erroneous measurement of the membrane deflection, therefore leading to a wrong estimation of the residual stress or cavity pressure. From Figs. 5.17 and 5.18 we can see that, in this work, the maximum measured deflection is, in all cases, less than the gap depth (3 μm).

The Young's modulus of the sealed membranes can be calculated by Eq. (5.4) [18], assuming the same value for Poisson's ratio for all layers:

$$E_c = \frac{\lambda \cdot E_{SiGe} \cdot t_{SiGe} + E_s \cdot t_s}{t_c} \tag{5.4}$$

where t is the thickness and the subscripts c and s represent the compound membrane and the sealing layer, respectively. The parameter λ (Sect. 5.6) is included to account for the reduction of the poly-SiGe membrane stiffness due to the release holes.

The Young's modulus of the poly-SiGe membrane and the different sealing materials was obtained from nanoindentation by using a continuous stiffness measurement (CSM) technique [26]. This technique consists of applying a small harmonic, high frequency amplitude force during indentation loading, and measuring the contact stiffness of the sample from the displacement response at the excitation frequency. The Young's modulus of the material is then derived from the contact stiffness. The Young's modulus of the compound membrane (E_c) is obtained from the measured values (Table 5.2) by applying Eq. (5.4). For the PECVD SiGe-sealed membranes, since no measurements were available, a Young's modulus $E = 140$ GPA was assumed [11]. For the porous μc-SiGe cover, a $E = 100$ GPa was considered.

Table 5.2 Measured young's modulus by nanoindentation

	SiGe (3.5μm)	SACVD oxide (0.9 μm)	HDP oxide (1 μm)	AlCu (1.5 μm)
E (GPa)	147±6	60±4	73±9	67±5

In parenthesis the thickness of the layer used in the measurements

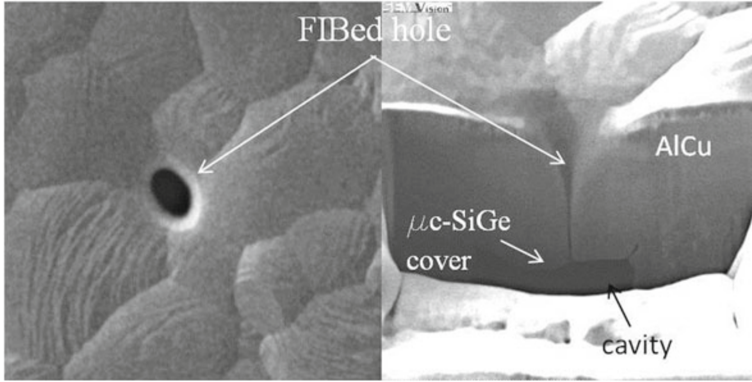

Fig. 5.19 *Top* view and cross-section pictures of a micro hole drilled in a μc-SiGe +AlCu sealed membrane

5.7.1 Membrane Behavior Under 0-Pressure Difference

The load-deflection technique can only be applied to membranes that remain flat without load. If the residual stress is compressive and large enough the membrane may buckle, leading to erroneous estimation of the cavity pressure [19, 27]. To verify if the membrane layers buckled or not, micro-venting holes of 1×1 μm^2 were drilled using a Focus Ion Beam (FIB) in some of the sealed membranes (Fig. 5.19). In this way a 0-pressure-difference reference is available. This hole made by FIB is so small that the effect on the global stress in the membrane can be neglected. Under a 0-pressure difference, thin film membranes show the following behavior: with tensile residual stress ($\sigma_0 > 0$) or weakly compressive stress ($\sigma_{crl} < \sigma_0 < 0$), the membrane is stable in the flat position. For a compressive stress greater than a critical stress σ_{crl}(given by (5.5) [28]) the membrane will buckle transversally without any external load

$$\sigma_{crl} = -4.363 \cdot \frac{E \cdot h^2}{(1 - v^2) \cdot L^2} \tag{5.5}$$

where E and v are the Young's modulus and Poisson's ratio, respectively, h is the membrane thickness and L is the membrane length.

Figure 5.20 shows the measured deflection of two membranes (one of them with a micro venting hole opened by FIB) sealed by a combination of μc-SiGe porous

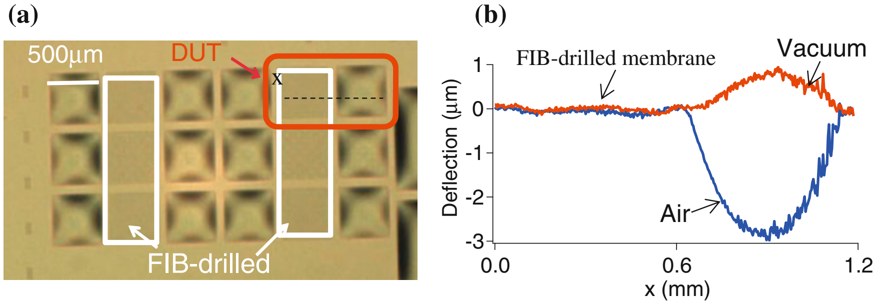

Fig. 5.20 *Top*-view picture of the membrane deflection for 18 cavities sealed with µc-SiGe porous layer and AlCu, in 6 of them (inside *white square*) **a** hole was drilled by FIB, **b** Membrane deflection measured by WLI on two membranes with and without the micro venting hole

layer and AlCu. All the FIB-drilled membranes studied in this work, except those sealed with HDP Si-oxide or SiGe, remain flat, which indicates an overall stress in the diaphragm either tensile or less compressive than the minimum critical stress (σ_{ctl} of the biggest membrane).

For HDP Si-oxide sealed membranes buckling was observed, which is not surprising considering the high compressive residual stress typically exhibited by HDP Si-oxide layers. However, only the larger membranes ($L = 300\,\mu$m) (Fig. 5.21a) buckled while the smaller membranes remain flat. This result indicates that the stress in the HDP-sealed membranes is compressive in the range ($\sigma_{ctl}(L = 300\,\mu\text{m})$, $\sigma_{ctl}(250\,\mu\text{m})$). From (5.5), the critical stress for $300\times300\ \mu\text{m}^2$ ($250\times250\ \mu\text{m}^2$) membranes sealed by HDP Si-oxide is -137.34 MPa (-197.76 MPa). On the other hand, the fact that the membranes of $500\times500\ \mu\text{m}^2$ sealed with SiGe exhibitted buckling indicates that the stress is more compressive than the critical stress of -43.51 MPa.

The exact value of the compressive residual stress in the buckled membranes can be extracted from the measured centre deflection of the FIB-drilled membranes by applying the expression given in [23]. The measured centre deflection is ~760 nm in the case of the FIBed $300\times300\ \mu\text{m}^2$ HDP Si-oxide sealed membrane and ~5µm for the SiGe-sealed $500\times500\ \mu\text{m}^2$ FIBed membrane. The obtained value for the residual stress is -139.2 MPa for the HDP Si-oxide sealed membrane, which falls into the predicted range. For the SiGe sealed membrane the residual stress is calculated to be -74.15 MPa.

To corroborate these results, nonlinear finite-element simulations of the buckling of a $300\times300\mu\text{m}^2$ membrane sealed with HDP were performed using COMSOL (Fig. 5.21). The total membrane thickness, Poisson's ratio and Young's modulus (from Eq. (5.4)) were set to 4.6 µm, 0.23 and 126.8 GPa respectively. The compressive residual stress was simulated thermally, following a similar approach as in [28]. In order to obtain a simulated deflection equal to the measured one (760 nm) a compressive stress $\sigma = -136.9$ MPa was found, close to the value predicted analytically.

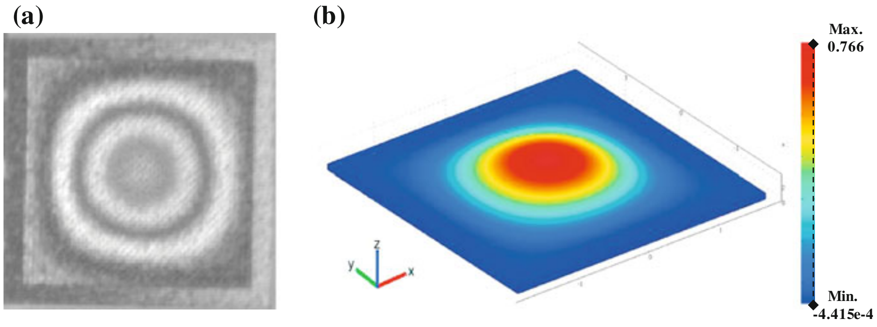

Fig. 5.21 Buckling of a $300 \times 300\,\mu m^2$ membrane sealed with HDP oxide under a 0-pressure difference. **a** Interferometric contour image and **b** simulation of the deflection under a thermally induced stress $\sigma = -136.9\,\mathrm{MPa}$

5.7.2 Cavity Pressure

It is important to determine the residual pressure inside the sealed cavity in order to predict the device performance. In thin-film packaging, the cavity pressure will affect the packaged device performance. For absolute pressure sensors, the pressure inside the sealed cavities supplies a reference for pressure measurements. Moreover, as mentioned in Sect. 5.1, the expansion of the gasses trapped inside the cavity will degrade the temperature dependence of the pressure sensors performance. Therefore it is, in general, preferred to have a vacuum-sealed cavity for pressure sensor applications as this will minimize the trapped gas effects. From the measurements discussed above, we can derive both the sealed-in pressure and the membrane stress for the different sealing approaches studied.

Since all the sealed membranes in this study (except for the $300 \times 300\,\mu m^2$ membranes sealed with HDP Si-oxide and the $500 \times 500\ \mu m^2$ membranes sealed with SiGe) remain flat under 0-differential pressure, the value of the sealed-in pressure (P_{in}) and residual stress of the compound membranes (σ_o) can be easily calculated from the load-deflection measurements by substituting in (5.1) E by E_c as calculated from (5.4), t by the total thickness of the composite membrane t_c and w_0 by the measured deflection. A constant value of Poisson's ratio $\nu_{SiGe} = 0.23$ is assumed for all compound membranes. Table 5.3 contains the obtained values. In the case of SiGe sealing, since no flat membranes are available, the cavity pressure was estimated from finite-element simulations (COMSOL). A negative value for σ_0 indicates a compressive stress. The relatively big uncertainty on the calculated values is mainly due to the limited accuracy in the optical measurements ($\pm 0.05\mu m$) and the control of the "vacuum" pressure (25 ± 5 kPa).

The values obtained for the overall stress in the sealed diaphragms (σ_o) are in good agreement with the observations made in Sect. 5.7.1 from the FIBed membranes. The compressive stress in the membrane with AlCu direct sealing is, as expected from the flat membranes after FIB hole drilling, below the critical pressure for buckling (Eq. (5.5)). The fact that the membranes sealed with AlCu only exhibitted compresive

Table 5.3 Overall stress and cavity pressure obtained from the load-deflection data for the different sealing techniques.

Sealing technique	Sealing layer	t_c (μm)	E_c (GPa)	σ_0 (MPa)	Pin (kPa)
Direct sealing	SACVD Si-oxide	4.6[a]	122.5	11±3	7±2
	AlCu	10	130.86	−50±10	<1
μc-SiGe porous layer	HDP Si-oxide[c]	4.6[b]	126.8	−130±10	20±5
	AlCu	2.89	121.3	90±5	40±2
	PECVD SiGe [1]	4	140	−75	60

[a] t_c= 3.5 μm membrane + 0.2 μm bottom SACVD + 0.9 μm top SACVD (Fig. 5.2a).
[b] t_c= 3.5 μm membrane + 0.2 μm porous layer + 0.9 μm HDP oxide (Fig. 5.10a).
[c] Sealing layer/membrane interface exposed

stress is a bit surprising considering that both SiGe and AlCu normally exhibit tensile stress. One possible explanation could be the strong reaction observed between SiGe and AlCu (see Fig. 5.6b), which might lead to volume changes and the creation of compressive stress. In the case of membranes sealed with a combination of porous layer and AlCu this reaction is not observed as the porous layer probably easily oxidizes and then acts as a barrier, preventing any reaction. The overall stress is tensile in that case as expected from the measured flat membranes under 0-differential pressure (see Fig. 5.20).

As it can be expected from the low deposition pressure, direct AlCu sealing results in (near) vacuum-sealed cavities. In Fig. 5.17 we can observe that the AlCu-only sealed membranes have a less negative deflection in air than the μc-SiGe+AlCu membranes. This may seem surprising since the found inside cavity pressure is much lower for the AlCu-only sealed membranes. But it can be easily explained considering that the total membrane thickness of the AlCu-only sealed membranes (11.5 μm) is around four times greater than the total thickness of the membranes sealed with μc-SiGe+AlCu (2.89 μm).

For SACVD oxide sealing a cavity pressure of around 7 kPa was found, considerably smaller than the value expected from the processing pressure, temperature and overall chemical reaction [29], when using the ideal gas law [30]. A possible explanation for this low sealed-in pressure could be the continued reaction of the trapped gases after sealing, which reduces the amount of gaseous products and reactants, and the absorption of the residual water vapor generated during the chemical reaction by the oxide layer inside the cavity [31].

For the cavities sealed using a porous μc-SiGe cover in combination with Si-oxide, AlCu or SiGe a quite high residual pressure was found. Of particular significance is the case of the cavities sealed with porous μc-SiGe and AlCu, for which a much higher sealed-in pressure (∼40 kPa) than for equivalent cavities sealed with only AlCu was found. One possible cause for this could be outgassing from the porous μc-SiGe cover. Indeed, recent experiments proved that as-deposited SiGe can outgas large quantities of hydrogen, water vapour and, in some cases, CO_2 [32]. The μc-SiGe cover, due to its porous texture, is expected to outgas even more. Moreover, during the sealing layer deposition, the porous cover will trap most of the outgassing from the SiGe cavity walls while during direct sealing the gasses can diffuse more

freely out of the cavity. Another explanation, proposed in [7], is the existence of a temporary leak path in the exposed interface between the porous μc-SiGe cover and the SiGe membrane. However this explanation would only be valid for the porous layer + HDP sealed cavities, since in the AlCu and SiGe cavities this interface is not exposed.

These results make it clear that, in case a low sealed-in pressure is desired, it is very important to ensure that the layers inside the cavity are properly outgassed before the cavity is sealed. This can be achieved, for example, by introducing an annealing step just before the deposition of the sealing material [32].

5.7.3 Long-Term Hermeticity

Long-term hermeticity tests were performed for the cavities with the lowest residual pressure (SACVD Si-oxide and AlCu sealed cavities). The hermeticity was investigated by measuring the membrane deflection at regular intervals of time. A difference in deflection after a certain period of time under the same pressure loading would indicate the presence of a leak path. Long-term deflection monitoring for 300×300 μm^2 SACVD sealed cavities and 500×500 μm^2 AlCu sealed cavities (Fig. 5.22) shows that there is no detectable change in cavity pressure over time.

A leak can be characterized by a standard leak rate r [33], defined as the quantity of dry air at 25 °C flowing through a leak or multiple leak paths per second when the high-pressure side is air at atmospheric pressure (101 kPa):

$$r = \frac{\Delta P \cdot V}{t} \tag{5.6}$$

where r is the standard leak rate in air, ΔP is the variation in sealed-in pressure, t is the time for the pressure change in seconds and V is the internal volume of the cavity. Assuming a 0.05μm resolution in the WLI measurement, which corresponds to a change in cavity pressure of ∼5.5 kPa for 300×300 μm^2 cavities (∼5.7 kPa for

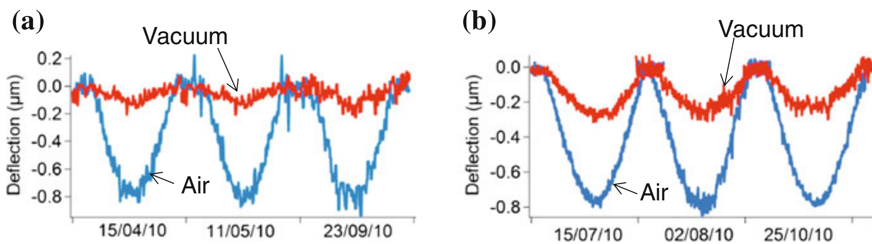

Fig. 5.22 Deflection measurement (1 membrane is shown) indicating long term hermeticity. In **a** the cavity is 300×300 μm^2 and the sealing layer is 900 nm SACVD oxide. In **b** the cavity is 500×500 μm^2 and sealing layer is 1.5 μm AlCu

$500 \times 500\ \mu m^2$ cavities), and applying Eq. (5.6), the obtained long-term hermeticity results point out a maximum possible leak rate (deflection resolution/monitoring time) of $\sim 1 \times 10^{-16}$ Pa·m^3/s ($\sim 5.5 \times 10^{-16}$ Pa·m^3/s) for SACVD Si-oxide (AlCu) sealing.

5.8 Summary and Conclusion

Two different techniques for the sealing of poly-SiGe microcavities by thin-film deposition have been presented: direct sealing and the use of an intermediate porous cover. Two different sealing materials were considered: Si-oxide and AlCu. The results were compared with SiGe sealing experiments from literature [11].

The experimental results prove that both Si-oxide and AlCu can provide short- and long-term air-tight sealing. SACVD Si-oxide offers an attractive and simple technique for the direct sealing of surface micromachined cavities, with a resulting cavity pressure below 10 kPa. Direct sealing with AlCu provides a near-vacuum sealed cavity and can be a promising technique for applications such as thin-film packaging or capacitive pressure sensors. For piezoresistive pressure sensors the use of AlCu as sealing layer is however not practical; extra isolation layer and/or extra processing steps might need to be introduced to avoid a short-circuit between different piezoresistors.

For applications where the deposition of sealing material inside the cavity is undesirable, the use of a porous μc-SiGe cover in combination with Si-oxide or AlCu has been proposed. This porous cover, although preventing the deposition of sealing material inside the cavity, resulted, for the cavities studied in this work, in a higher sealed-in pressure. In order to use this porous cover it is important to ensure proper outgassing of the materials used inside the cavity and to avoid an exposed SiGe membrane/ μc-SiGe interface.

After all these experiments SACVD Si-oxide was the selected sealing material for the development of the pressure sensor. Sealing with SACVD Si-oxide is simple and efficient, since relatively thin layers are enough to seal the cavities. It also results in a smooth sealed surface that will facilitate further processing (like, for example, the deposition/patterning of the metal lines connecting the piezoresistors). Moreover the Si-oxide sealing layer can be used as isolation between the membrane, the different piezoresistors and the metal interconnects. The poly-SiGe cavities sealed with SACVD Si-oxide also exhibited marginally tensile stress, very attractive for pressure sensor applications. On the other hand, SACVD Si-oxide presents two important drawbacks. The first inconvenience is the relatively high sealed-in pressure that can pose a problem in low-pressure applications. For our test devices this is however not a big issue. A second important drawback of SACVD Si-oxide as sealing layer is the big CTE mismatch with the poly-SiGe membrane that will compromise the temperature stability of the pressure sensor performance. From CTE point of view the most interesting sealing material considered would be SiGe. In this way an all-SiGe (membrane, piezoresistors and sealing layers) pressure sensor can be obtained.

However, if SiGe is to be used as sealing material, further developments are needed to tune the stress to obtain an overall marginally tensile stress and avoid buckling. Also, a new recipe to have an undoped SiGe sealing layer would be required to avoid an unwanted electrical connection between the interconnects, the membrane and the piezoresistors.

References

1. K. Petersen, P.W. Barth, J. Poydock, J. Brown, J. Mallon, J. Bryaek, Silicon fusion bonding for pressure sensors, in *Proceeding of the IEEE Solid-State Sensor and Actuator Workshop*, Freemont (CA), 6–9 June 1988, pp. 144–147
2. H. Guckel, D.W. Burns, Planar processed polysilicon sealed cavities for pressure transducer arrays, in *Proceeding of IEDM*, 1984, pp. 223–225
3. C.H. Mastrangelo, R.S. Muller, S. Kumar, Microfabricated incandescent lamps. Appl. Opt. **30**, 868–873 (1993)
4. L. Lin, R.T. Howe, A.P. Pisano, Microelectromechanical filters for signal processing. J. Microelectromech. Syst. **7**, 286–294 (1998)
5. C. Liu, Y. Tai, Sealing of micromachined cavities using chemical vapor deposition methods: characterization and optimization. J. Microelectromech. Syst. **8**, 135–145 (1999)
6. M. Bartek, J.A. Foerster, R.F. Wolffenbuttel, Vacuum sealing of microcavities using metal evaporation. Sens. Actuators A , **61**, 364–368 (1997)
7. B. Guo, L. Wen, P. Helin, G. Claes, A. Verbist, R. Van Hoof, B. Du Bois, J. De Coster, I. De Wolf, A. Hadi Shahar, Y. Li, H. Cui, M. Lux, G. Vereecke, H.A.C. Tilmans, L. Haspeslagh, S. Decoutere, H. Osman, R. Puers, S. Severi, A. Witvrouw, Above-IC generic poly-SiGe thin film wafer level packaging and MEM device technology: application to accelerometers, in *Proceeding og the IEEE 24th International Conference on Micro Electro Mechanical Systems (MEMS)*, Mexico, 23–27 Jan 2011, p. 355
8. Y. Naito, P. Helin, K. Nakamura, J. De Coster, B. Guo, L. Haspeslagh, K. Onishi, H. A. C. Tilmans, High-Q torsional mode si triangular beam resonators encapsulated using SiGe thin film, *2010 IEEE International Electron Device Meeting (IEDM)*, pp. 7.1.1–7.1.4
9. M. Gromova, K. Baert, C. Van Hoof, A. Mehta, A. Witvrouw, The novel Use of low temperature hydrogenated microcrystalline silicon germanium (μcSiGe:H) for MEMS applications. Microelectron. Eng. **76**(1–4), 266–271 (2004)
10. G. Bryce, S. Severi, R. van Hoof, B. Guo, E. Kunnen, A. Witvrouw, S. Decoutere, Development, optimization and evaluation of a CF4 pre-treatment process to remove unwanted interfacial layers in stacks of CVD and PECVD polycrystalline Silicon-Germanium for MEMS applications. ECS Trans. **28**, 79–90 (2010)
11. G. Claes, Poly-silicon germanium thin-film package: study of structural features enabling CMOS-MEMS integration, Ph. D. thesis, Katholieke Universiteit Leuven, July, 2011
12. G.G. Stoney, The tension of thin metallic films deposited by electrolysis. Proc. Roy. Soc. Lond. A **82**, 172–175 (1909)
13. R. Arghavani, Z. Yuan, N. Ingle, K-B Jung, M. Seamons, S. Venkataraman, V. Banthia, K. Lilja, P. Leon, G. Karunasiri, S. Yoon, and A. Mascarenhas, Stress management in Sub-90-nm transistor architecture. IEEE Trans. Electr. Devices, **51**(10), 1740–1743 (2004)
14. A. Witvrouw, J. Proost, B. Deweerdt, Ph Roussel, K. Maex, Stress relaxation in Al-Si-Cu thin films and lines. Mat. Res. Soc. Symp. Proc. **356**, 441–446 (1995)
15. I. de Wolf, J. de Coster, O. Varela Pedreira, L. Haspeslagh, A. Witvrouw, Wafer level characterization and failure analysis of microsensors. Proc. IEEE Sens. **26–29**, 144–147 (Oct. 2009)
16. O. Varela Pedreira, T. Lauwagie, J. de Coster, L. Haspeslagh, A. Witvrouw, I. de Wolf, High throughput measurement techniques for wafer level yield inspection of MEMS devices, in *Proceeding of the SPIE 9th International Symposium LM*, vol. 7155 715 50M-1–11, 2008

17. M. Zecchino, Characterazing MEMS devices through transparent media (2010), http://www.bruker-axs.com/
18. O. Tabata, K. Kawahata, S. Sugiyama, I. Igarashi, Mechanical property measurements of thin films using load-deflection of composite rectangular membrane, in *Proceeding of the MEMS 1989*, pp. 152–156
19. M.G. Allen, M. Mehregany, R.T. Howe, S.D. Senturia, Microfabricated structures for the in situ measurement of residual stress, young's modulus and ultimate strain of thin films. Appl. Phys. Lett. **51**, 241–243 (1987)
20. S.D. Senturia, *Microsystems Design* (Kluwer Academic Publisher, Norwell, 2000)
21. D. Maier-Schneider, J. Maibach, E. Obermeier, A new analytical solution for the load-deflection of square membranes. J. Microelectromech. Syst. **4**, 238–241 (1995)
22. D. Maier-Schneider, A. Köprülülü, S. Ballhausen Holm, E. Obermeier, Elastic properties and microstructure of LPCVD polysilicon films. J. Micromech. Microeng. **6**, 436–446 (1996)
23. COMSOL multiphysics, www.comsol.com
24. A. Partridge, A. E. Rice, T.W. Kenny, New thin film epitaxial polysilicon encapsulation for piezoresistive accelerometers, in *Proceeding of the IEEE 14th International Conference on Micro Electro Mechanical Systems (MEMS)*, pp. 54–59, 2001
25. T. Kramer, O. Paul", Postbuckled micromachined square membranes under differential pressure. J. Micromech. Microeng. **12**, 475–478 (2002)
26. X. Li, B. Bhushan, A review of nanoindentation continuous stiffness measurement technique and its applications. Mater. Character. **48**, 11–36 (2002)
27. M.A. Huff, A.D. Nikolich, M.A. Schmidt, Design of sealed cavity microstructures formed by silicon wafer bonding. J. Microelectromech. Syst. **2**, 74–81 (1993)
28. V. Ziebart, O. Paul, H. Baltes, Strongly buckled square micromachined membranes. J. Microelectromech. Syst. **4**, 423–32 (1999)
29. K. Fujino, Y. Nishimoto, N. Tokumasu, K. Maeda, Silicon dioxide deposition by atmospheric pressure and low-temperature CVD Using TEOS and Ozone. J. Electrochem. Soc. **137**, 2883–2887 (1990)
30. R. Legtenberg, H.A.C. Tilmans, Electrostatically driven vacuum-encapsulated polysilicon resonators Part I. Design and fabrication. Sens. Actuators A **45**, 57–66 (1994)
31. J.A. Voorthuyzen, K. Keskin, P. Bergveld, Investigations of the surface conductivity of silicon dioxide and methods to reduce it. Surf. Sci. **187**, 201–211 (1987)
32. B. Wang, S. Tanaka, B. Guo B, G. Vereecke, S. Severi, A. Witvrouw, M. Wevers, I. De Wolf, Outgassing studies of thin-films used for poly-SiGe based vacuum packaging of MEMS. Microelectron. Reliab. **51**(9–11), 1878–1881 (2011)
33. Q. Li, H. Goosen, F. van Keulen, J. van Beek, G. Zhang, Assessment of testing methodologies for thin-film vacuum MEMS packages. Microsyst. Technol. **15**, 161–168 (2009)